Spring Land Temperature in Tibetan Plateau and Global-Scale Summer Precipitation
Initialization and Improved Prediction

Yongkang Xue, Ismaila Diallo, Aaron A. Boone, Tandong Yao, Yang Zhang, Xubin Zeng, J. David Neelin, William K. M. Lau, Yan Pan, Ye Liu, Xiaoduo Pan, Qi Tang, Peter J. van Oevelen, Tomonori Sato, Myung-Seo Koo, Stefano Materia, Chunxiang Shi, Jing Yang, Constantin Ardilouze, Zhaohui Lin, Xin Qi, Tetsu Nakamura, Subodh K. Saha, Retish Senan, Yuhei Takaya, Hailan Wang, Hongliang Zhang, Mei Zhao, Hara Prasad Nayak, Qiuyu Chen, Jinming Feng, Michael A. Brunke, Tianyi Fan, Songyou Hong, Paulo Nobre, Daniele Peano, Yi Qin, Frederic Vitart, Shaocheng Xie, Yanling Zhan, Daniel Klocke, Ruby Leung, Xin Li, Michael Ek, Weidong Guo, Gianpaolo Balsamo, Qing Bao, Sin Chan Chou, Patricia de Rosnay, Yanluan Lin, Yuejian Zhu, Yun Qian, Ping Zhao, Jianping Tang, Xin-Zhong Liang, Jinkyu Hong, Duoying Ji, Zhenming Ji, Yuan Qiu, Shiori Sugimoto, Weicai Wang, Kun Yang, and Miao Yu

ABSTRACT: Subseasonal-to-seasonal (S2S) precipitation prediction in boreal spring and summer months, which contains a significant number of high-signal events, is scientifically challenging and prediction skill has remained poor for years. Tibetan Plateau (TP) spring observed surface temperatures show a lag correlation with summer precipitation in several remote regions, but current global land–atmosphere coupled models are unable to represent this behavior due to significant errors in producing observed TP surface temperatures. To address these issues, the Global Energy and Water Exchanges (GEWEX) program launched the "Impact of Initialized Land Temperature and Snowpack on Subseasonal-to-Seasonal Prediction" (LS4P) initiative as a community effort to test the impact of land temperature in high-mountain regions on S2S prediction by climate models: more than 40 institutions worldwide are participating in this project. After using an innovative new land state initialization approach based on observed surface 2-m temperature over the TP in the LS4P experiment, results from a multimodel ensemble provide evidence for a causal relationship in the observed association between the Plateau spring land temperature and summer precipitation over several regions across the world through teleconnections. The influence is underscored by an out-of-phase oscillation between the TP and Rocky Mountain surface temperatures. This study reveals for the first time that high-mountain land temperature could be a substantial source of S2S precipitation predictability, and its effect is probably as large as ocean surface temperature over global "hotspot" regions identified here; the ensemble means in some "hotspots" produce more than 40% of the observed anomalies. This LS4P approach should stimulate more follow-on explorations.

KEYWORDS: Atmosphere; Atmosphere-land interaction; Ensembles; Numerical weather prediction/forecasting; General circulation models; Model initialization

AFFILIATIONS: **Xue, Diallo, Neelin, and Nayak**—University of California, Los Angeles, Los Angeles, California; **Boone and Ardilouze**—CNRM, Université de Toulouse, Météo-France, CNRS, Toulouse, France; **Yao, X. Pan, Li, and W. Wang**—Institute of Tibetan Plateau Research, Chinese Academy of Sciences, Beijing, China; **Y. Zhang, Y. Pan, Guo, and J. Tang**—School of Atmospheric Sciences, Nanjing University, Nanjing, China; **Zeng and Brunke**—The University of Arizona, Tucson, Arizona; **Lau**—Earth System Science Interdisciplinary Center, University of Maryland, College Park, College Park, Maryland; **Liu**—University of California, Los Angeles, Los Angeles, California, and Pacific Northwest National Laboratory, Richland, Washington; **Q. Tang and Xie**—Lawrence Livermore National Laboratory, Livermore, California; **Oevelen**—International GEWEX Project Office, George Mason University, Fairfax, Virginia; **Sato and Nakamura**—Hokkaido University, Sapporo, Japan; **Koo**—Korea Institute of Atmospheric Prediction Systems, Seoul, South Korea; **Materia and Peano**—Climate Simulation and Prediction, Fondazione Centro Euro-Mediterraneo sui Cambiamenti Climatici, Bologna, Italy; **Shi**—National Meteorological Information Center, China Meteorological Administration, Beijing, China; **J. Yang, Qi, Fan, and D. Ji**—Beijing Normal University, Beijing, China; **Z. Lin, Feng, Zhan, and Qiu**—Institute of Atmospheric Physics, Chinese Academy of Sciences, Beijing, China; **Saha**—Indian Institute of Tropical Meteorology, Pune, India; **Senan, Vitart, Balsamo, and Rosnay**—European Centre for Medium-Range Weather Forecasts, Reading, United Kingdom; **Takaya**—Meteorological Research Institute, Japan Meteorological Agency, Tsukuba, Japan; **H. Wang and Zhu**—National Center for Environmental Prediction, College Park, Maryland; **H. Zhang**—National Meteorology Center, Chinese Meteorological Administration, Beijing, China; **M. Zhao**—Bureau of Meteorology, Melbourne, Victoria, Australia; **Chen**—University of California, Los Angeles, Los Angeles, California, and School of Atmospheric Sciences, Nanjing University, Nanjing, China; **S. Hong**—Korea Institute of Atmospheric Prediction Systems, Seoul, South Korea, and NOAA/ESRL, and Cooperative Institute for Research in Environmental Sciences, University of Colorado Boulder, Boulder, Colorado; **Nobre and Chou**—Instituto Nacional de Pesquisas Espaciais, São José dos Campos, Cachoeira Paulista, Brazil; **Qin**—Lawrence Livermore National Laboratory, Livermore, California, and Tsinghua University, Beijing, China; **Klocke**—Max Planck Institute for Meteorology, Hamburg, Germany; **Leung and Qian**—Pacific Northwest National Laboratory, Richland, Washington; **Ek**—National Center for Atmospheric Research, Boulder, Colorado; **Bao**—LASG, Institute of Atmospheric Physics, Chinese Academy of Sciences, Beijing, China; **Y. Lin and K. Yang**—Tsinghua University, Beijing, China; **P. Zhao**—Chinese Academy of Meteorological Sciences, China Meteorological Administration, Beijing, China; **Liang**—University of Maryland, College Park, College Park, Maryland; **J. Hong**—Yonsei University, Seoul, South Korea; **Z. Ji**—Sun Yat-Sen University, Guangzhou, China; **Sugimoto**—Japan Agency for Marine-Earth Science and Technology, Yokosuka, Japan; **Yu**—Nanjing University of Information Science and Technology, Nanjing, China

Subseasonal-to-seasonal (S2S) precipitation prediction in boreal spring and summer months, despite including large number of high-impact events, such as droughts/floods, has remained poor for years. It has been cited in the current joint World Weather Research Programme (WWRP) and World Climate Research Programme (WCRP) S2S Prediction Project, which aims to improve understanding and forecast accuracy at the S2S time scale, as a "weather–climate prediction desert" with a high priority (Robertson et al. 2018; Merryfield et al. 2020). Robust land initialization and model configuration are critical to this effort yet remain scientifically challenging. The land's role in the climate system at various scales has been the subject of much research since the 1970s. A few land surface attributes, such as albedo, soil moisture, leaf area index, vegetation, and aerosols in snow have been extensively investigated to explore their roles in land–atmosphere interactions (Charney et al. 1977;

Shukla and Mintz 1982; Barnett et al. 1989; Zeng et al. 1999; Koster et al. 2004; Xue et al. 2010; Qian et al. 2011; Materia et al. 2022). However, most studies of land–atmosphere interactions have been limited by a lack of observational data and tend to focus on local feedbacks (Koster et al. 2004). The potential for land surface processes to improve S2S precipitation prediction, especially of droughts and floods, has not been extensively explored in previous land–atmosphere interaction studies.

Ocean state is well known to play a major role in modulating Earth's climate. The linkage of hydrological events to sea surface temperature (SST) anomalies, such as El Niño and La Niña, has been used to predict climate events with useful skill at long lead times ranging from a few months to a few years (Barlow et al. 2001; Schubert et al. 2009; Seager et al. 2014; Meehl et al. 2014). It has also been recognized that the Madden–Julian oscillation (MJO) provides an important source of S2S predictability (Vitart 2017; Woolnough 2019). However, studies have also consistently shown that the SST only partially explains climate predictability (Scaife et al. 2009; Xue et al. 2016a; Orth and Seneviratne 2017).

Recent preliminary studies based on observational data and modeling have indicated that spring land temperature in the Rocky Mountains and the Tibetan Plateau (TP) could affect summer drought/flood in their respective downstream regions with a magnitude comparable to the SST effect and atmospheric internal variability (Xue et al. 2016b, 2018). Although land surface 2-m air temperature (T2m) measurements have the best quality and longest record among various land surface variables with global coverage, their application in land–atmosphere interaction studies, S2S prediction in particular, has largely been overlooked.

Encouraged by the preliminary results, the Global Energy and Water Exchanges (GEWEX) program launched an initiative in 2018, the "Impact of Initialized Land Temperature and Snowpack on Subseasonal to Seasonal Prediction" (LS4P), as a community effort to test the impact of initializing land surface temperature (LST) and subsurface soil temperature (SUBT) in high-mountain regions in climate models on S2S prediction (Xue et al. 2021). More than 40 institutions, including many major climate centers worldwide, are participating in this project. Because of the high elevation of the TP, its significant areal coverage, and the comprehensive field measurements by the Third Pole Environment (Li et al. 2020) and other projects (Zhao et al. 2018) that span more than a decade, the LS4P Phase I focuses on the first-order effects most related to TP land temperature. The TP LST and SUBT are used as predictors of spring/summer precipitation events. The year 2003, when extreme summer drought/flood occurred in East Asia after a very cold spring in the TP, is the focal case (Xue et al. 2021). A case study focused on a specific year has been widely used in past exploratory studies in new concept development (Charney et al. 1977; Trenberth et al. 1988; Koster et al. 2004). The LS4P focuses on process understanding and predictability. As such, it is different from, and complements, other international projects that focus on the operational S2S prediction (Kirtman et al. 2014; Pegion et al. 2019). This article presents promising observational and modeling results from the LS4P explorations of new directions, which are related to the importance of land temperature memory for S2S prediction.

Studies have shown that the land temperature has substantial memory. Hu and Feng (2004) have found that the soil enthalpy anomaly in the top 20–50-cm soil column in the northwest United States can persist for up to 2–3 months. In another study (Liu et al. 2020), using the observational soil temperature data over the TP, which includes the soil temperature measurements extending downward to a soil depth of 3.2 m, they found that the anomalous LST in the TP can be sustained for several seasons, and it is accompanied by persistent SUBT as well as snow anomalies. Our research (Xue et al. 2021) also shows that the monthly T2m anomalies over the TP and the Rocky Mountains during years with cold and warm conditions in May can persist for several months, especially during the spring. This observational evidence suggests that the LST could be a source of memory for S2S prediction.

In this study, observed T2m records are used to examine possible relationships between the TP T2m and global precipitation and to identify the locations (hotspots) where the initialization of TP May land temperatures may enhance June precipitation prediction skill. The differences in observed May T2m between the five coldest and the five warmest Mays in the TP during the period 1981–2015 are shown in Fig. 1a. The years were selected based on the Tibetan Plateau index (TPI), which is defined as the averaged T2m anomaly over the region bounded by 29°–37°N, 86°–98°E (Fig. ES1 in the online supplemental material; https://doi.org/10.1175/BAMS-D-21-0270.2). All but two of these selected years had temperature anomalies above one standard deviation of the TP T2m interannual variability (0.77°C). When the TP spring was very cold, there was a corresponding warm anomaly in the western North America, mainly over the Rocky Mountain region (Fig. 1a), which will be further discussed below. This opposite-phase relationship is not sensitive to the selected years. Supplemental Fig. ES1 shows the differences of cold and warm months of May, which are selected based on a 0.5 standard deviation (total: 24 years). The opposite T2m spatial anomaly pattern between the TP and the Rocky Mountains is still the same. In fact, the anomaly patterns over Alaska and northwest Canada are also similar.

Figure 1b shows the June precipitation difference between the same years as in Fig. 1a. The dry southern Yangtze River basin and wet area to the north are evident (Fig. 1b), consistent with previous analyses (Xue et al. 2018). Interestingly, in North America, there was a
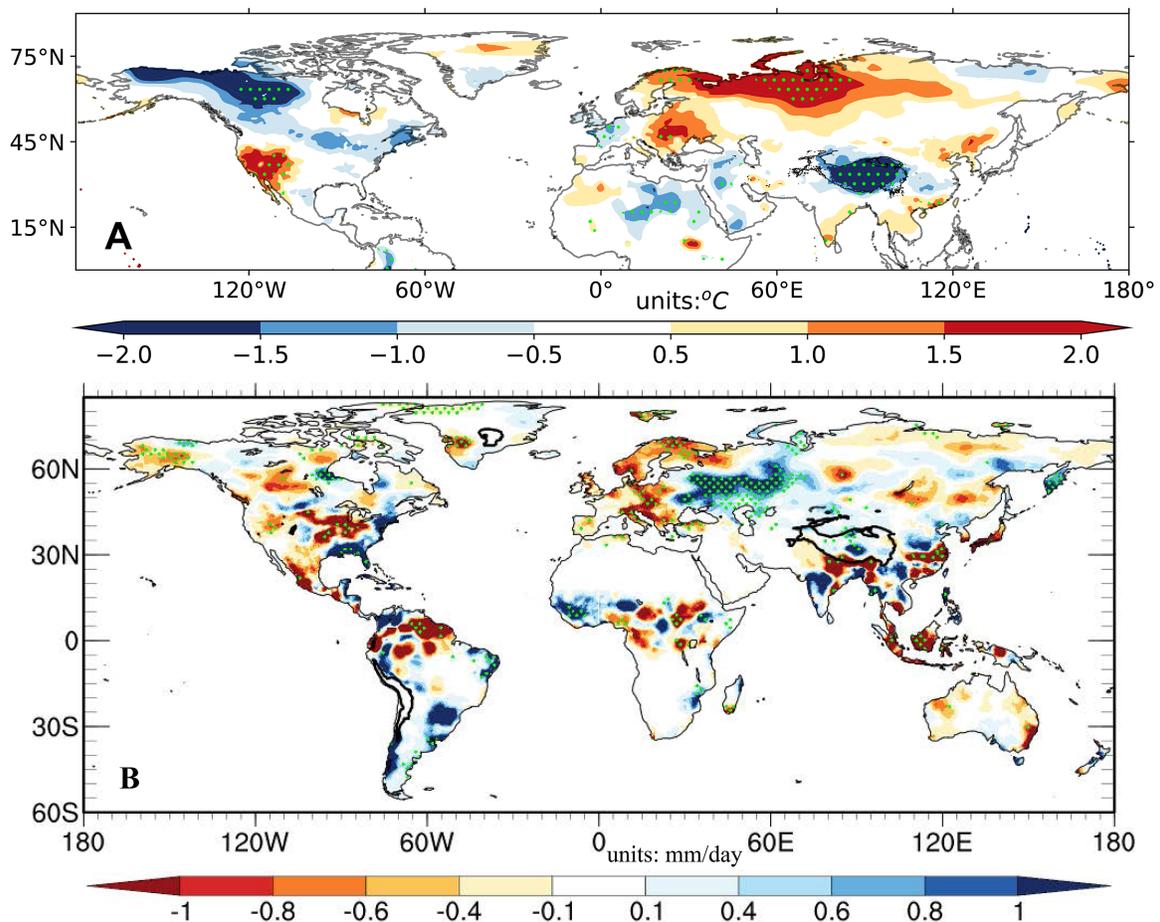

Fig. 1. Observed differences between the five coldest and the five warmest Mays in the Tibetan Plateau. (a) The difference in May T2m (°C) and (b) the difference in June precipitation for the same years. Note that the stippling in both figures denote statistical significance at the *p* < 0.1 level. In this study, the Chinese Meteorological Administration (CMA) T2m data (Han et al. 2019), which consist in 80 stations over the TP and more than 2,400 stations over all of China, are used over China. The Climate Anomaly Monitoring System (CAMS) T2m data are used elsewhere. The Climate Research Unit (CRU) data are used for precipitation over globe.

relatively wet southern Great Plains and an opposite anomaly to the north. This anomalous precipitation pattern is consistent with the warm May in the western United States (Fig. 1a), a relationship that has also been confirmed in past studies (Xue et al. 2016b, 2018). Moreover, the June precipitation anomalies are evident in other regions, such as Southeast and Northeast Asia, West Africa, Central America, and northern South America. To further confirm these lag relationships, we conducted regression analyses using data from 1980 to 2011 and produced consistent results (Fig. ES2 compared to Fig. 1). These results suggest that the lag relationship between TP May T2m and June precipitation anomalies is likely not limited to East Asia but extends through teleconnections to several remote regions. This finding motivated our use of multiple Earth system models (ESMs) to examine whether such lag relationships indeed suggest causality.

Two pairs of experiments with 16 state-of-the-art LS4P ESMs (Table ES1) have been conducted. In the first experiment (referred to as control run), we evaluate whether the ESMs can properly produce the observed TP T2m anomaly in May 2003 and the June precipitation anomaly. Each ESM model conducts about 2-month simulation from late April or early May through June 2003 with their normal setting for an S2S prediction for model initial conditions and land/ocean surface boundary conditions. All these ESMs except for one used specified SST as the ocean boundary condition. At least six ensemble members are required for each ESM. The results, however, show large biases (errors) in May 2003 T2m over the TP and June precipitation over many parts of the world (Xue et al. 2021). For example, 12 ESMs with a warm bias over the TP have a mean bias of +1.54°C and 4 ESMs with a cold bias have a mean bias of –1.07°C. The interannual standard deviation of T2m over the TP, however, was only 0.77°C. Meanwhile, the LS4P ESMs also have large precipitation biases over many regions (Fig. ES3). For instance, the southern Yangtze River basin in June 2003 experienced severe drought, with –1.41 mm day^{-1} of precipitation anomaly averaged over the region, while the 16 ESM ensemble mean shows a wet bias of +1.0 mm day^{-1}.

To alleviate the ESMs' May TP T2m bias and to generate the observed cold TP spring anomaly, we introduce an innovative approach to initializing the LST/SUBT over the TP. The technical aspect of the initialization set up has been presented in Xue et al. (2021). Land initialization and configuration have been identified as one of the major avenues for improving S2S prediction (Merryfield et al. 2020). Note that LST and SUBT can be initialized because they are prognostic variables, while T2m is a diagnostic variable meaning it cannot be used for initialization. However, the observed T2m is used as a proxy for initializing LST and SUBT because T2m and LST are very close in magnitude and variability, and LST and SUBT are highly correlated (Hu and Feng 2004; Liu et al. 2020).

After adjusting the LST/SUBT initial conditions based on each model's T2m bias and observed anomaly over the TP (Xue et al. 2021), a second experiment (referred to as the sensitivity run) is conducted using the new LST/SUBT initial condition for each model over the TP, with all other initial and boundary conditions and ensemble members identical to the first experiment.

Since the LS4P models have either warm or cold T2m biases over the TP in their control run, the intention of the initialization is to reduce the warm or cold bias in order to reproduce the observed May T2m anomaly over the TP. As such, for those models having control runs with a warm bias (referred to as warm case)/cold bias (referred to as cold case) over the TP, in the sensitivity run, we impose a land temperature mask over the TP only in the initialization step to make the surface temperature cooler/warmer compared to their respective control runs, and we refer to those sensitivity runs as the cold case/warm case, respectively. That being said, the individual member of the cold cases or warm cases could be from either control run or the sensitivity run depending on the model's initial bias (cold or warm) in the control run or the imposed mask (cold or warm) in the sensitivity run. A schematic diagram is displayed in Fig. ES4
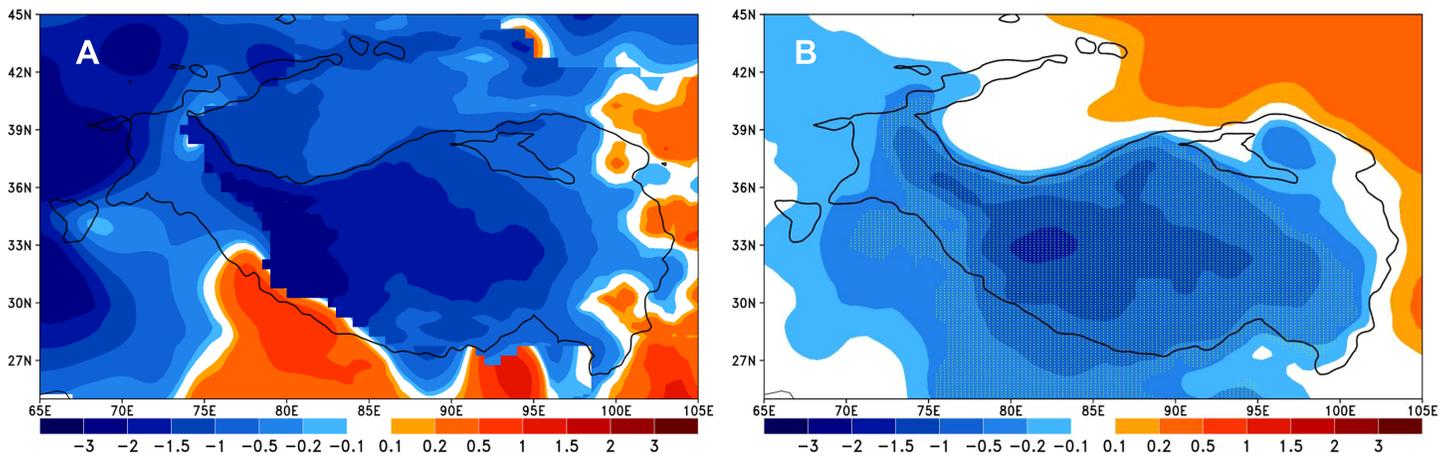
Fig. 2. Comparison between the observed May 2003 T2m anomaly and the model simulated LST/SUBT initialization effect (°C). (a) The observed May T2m difference between year 2003 and the mean value for 1981–2010. (b) The ensemble-mean T2m difference between the cold and warm cases (see text) produced after the LST/SUBT initialization. Note that the stippling in (b) indicates statistical significance at the *p* < 0.05 level.

to delineate this experimental design. Please note that the warm case just has relatively warmer temperature over the TP compared to the cold case as indicated in the schematic diagram Fig. ES4. The warm or cold case does not necessarily represent the warm year or cold year over TP. We expect the difference between the ensemble means for these cold cases and warm cases to generate, to some degree, the observed May 2003 cold TP T2m anomaly.

The LS4P objective is to examine whether the observed cold May 2003 TP anomaly causes the observed remote June precipitation anomalies over hotspots worldwide. For this purpose, the differences between the cold case and the warm case of the 16 ESM ensemble means are presented in this article to show 1) whether the adjusted LST and SUBT initial conditions produce, to some degree, the observed cold May T2m anomaly over the TP, and 2) how the simulated cold TP influences the spatial patterns and the magnitude of global June precipitation anomalies, compared with observations (see Figs. 1b and 3a and Fig. ES2b). The areas with a significant June precipitation impact due to the TP May cold temperature, that are also consistent with the observations, are defined as hotspots.

This paper as a *BAMS* article is meant to shed light on the new development and provide a new and potentially far-reaching perspective to spark the readers' interest in further exploration. Here we present only the key findings. Figure 2a shows the observed May 2003 T2m anomaly (relative to the climatology) over the TP, but the current LS4P ESMs have substantial bias there as demonstrated in Fig. ES3a. Figure 2b shows that after implementing the novel LST/SUBT initialization over the TP, the ensemble-mean T2m difference between cold cases and warm cases can reasonably reproduce the cold May surface temperature anomaly over the TP, although the amplitude is slightly underestimated (about −0.82°C versus the −1.41°C observed anomaly). In fact, after LST/SUBT initialization, the difference is much closer to the observed anomaly during the early May, when the model starts the simulation. On May 1, the difference is −1.1°C. However, current state-of-the-art ESMs are unable to fully preserve the memory from initialized LST anomalies due to deficiencies in model parameterizations and in the reanalysis data that provide unbalanced initial atmospheric/land conditions (Xue et al. 2021). A more detailed discussion on this issue will be presented in an LS4P paper in a special issue of *Climate Dynamics*, which is expected to be published in 2023. Nevertheless, a significant cold anomaly over the TP is produced (Fig. 2b). In the model ensemble, the teleconnected impact of this on June precipitation is substantial over many parts of the world (compare Figs. 3a and 3b). Figure 3a shows the observed June precipitation anomaly. Consistent with Fig. 2, Fig. 3 also uses the climatology as reference. In Fig. 3a, in addition to the well-known drought in the southern Yangtze River basin, there are many wet/dry
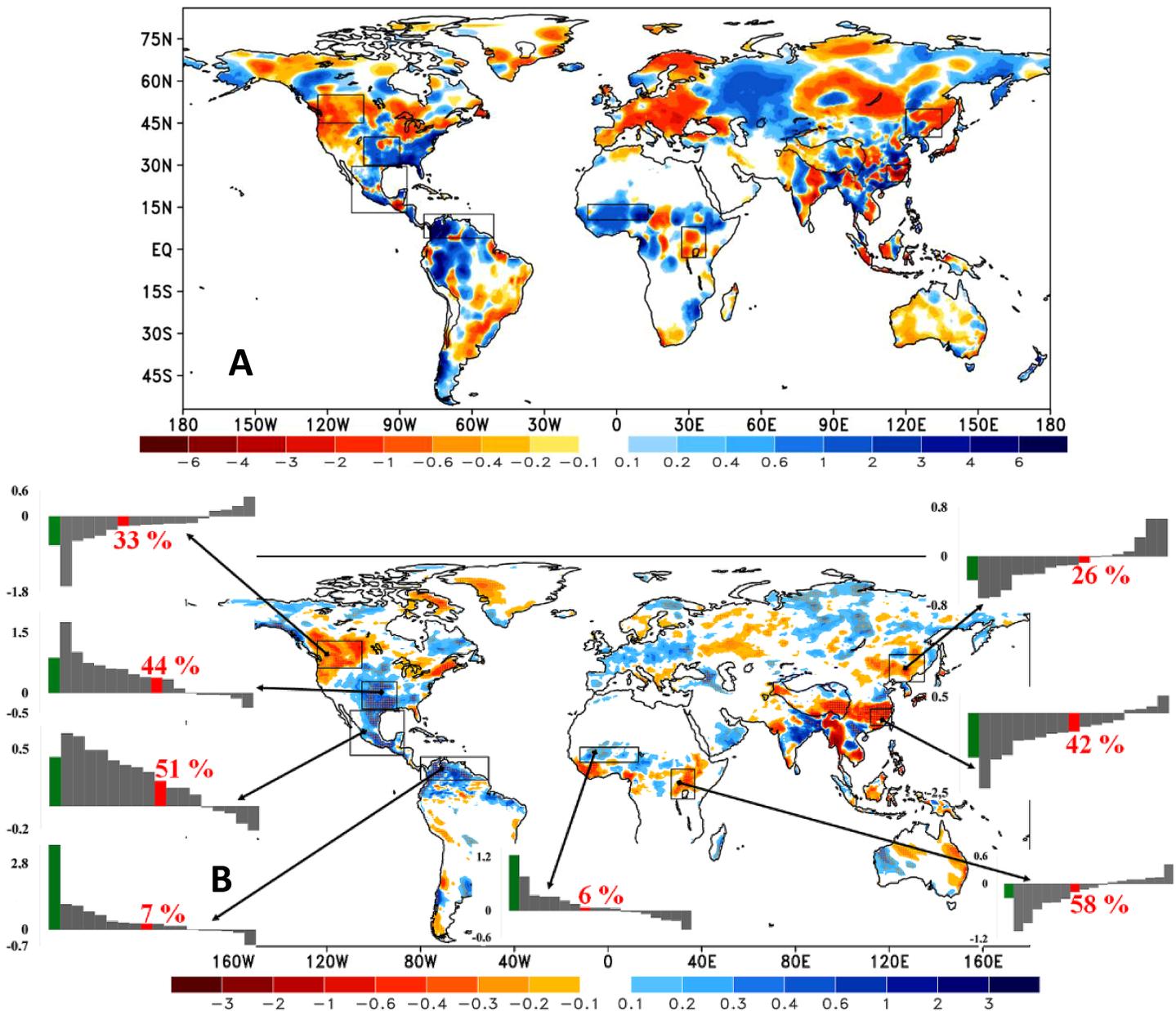
Fig. 3. Comparison of observed and simulated June 2003 precipitation anomaly. (a) Observed difference between year 2003 and the mean of 1981–2010. (b) Model-simulated precipitation anomalies (mm day^{-1}) after producing the cold TP anomaly shown in Fig. 2b. Notes: 1) Boxes indicate the hotspots; 2) gray bars denote different models and are arranged in a descending order for each region, the green bar is observation, and the red bar is the ensemble mean in each hotspot; 3) simulated percentages of observed anomalies from the ensemble mean are shown in red font above or below the red bars.

anomalies over the globe. Based on the definition of hotspots in this paper discussed above, by comparison to observations and simulations, eight hotspots (the boxes in Fig. 3b, Table ES2) are identified with a significant precipitation difference ($p < 0.10$).

In addition to the expected difference in the Yangtze River basin, regions of North and Central America show the largest impacts. For these hotspots, very few models produce anomalies that are different in sign compared to the observations (inserted bar graphs in Fig. 3b). For the hotspots in tropical regions, such as the Sahel, East Africa, and northern South America, model uncertainties are relatively large. The regions with observed anomalies in Fig. 1b and where the hotspots in Fig. 3b are consistent over Asia, North and Central America, and the Sahel, the lag relations for these regions appear to represent cause and effect. For northern South America, however, they have opposite signs, and eastern Africa does not appear clearly in Fig. 1b. This is likely because the winter season of 2002/03 is associated with

El Niño, and May and June 2003 were quite cold over the east Pacific (Xue et al. 2018), which presents a climate with quite different features compared to the mean climatology shown in Fig. 1. With only one case for 2003, it is hard to assess whether the difference between the climatology and the year 2003 over northern South America is a manifestation of the ENSO and the TP LST interaction. Further investigations are needed. But when we compare Fig. 3a and Fig. 3b, it is clear that Fig. 3b produces signals in broad agreement with the 2003 observation for these two hotspots.

There are two issues that need further investigation: 1) The ensemble-mean-produced T2m difference (Fig. 2b) is smaller than the observed anomaly (Fig. 2a). Would this deficiency cause an underestimation of the TP T2m effect? 2) In some areas, the ensemble mean produces a significant June precipitation difference (Fig. 3b), such as in western Australia and western Europe, but with the opposite sign compared to the observation (Fig. 3a). Is this due to a model deficiency in its ability to produce the full TP T2m anomaly and/or correct precipitation anomaly, and/or some other processes involved? More investigation is necessary.

Figure 3b suggests a linkage between the TP spring LST/SUBT and summer precipitation over North America. In fact, after generating a cold TP (Fig. 2b), a warm western United States is produced (not shown), consistent with the results in Fig. 1a. This should contribute to a wet southern Great Plains (Xue et al. 2018). Lau and Weng (2002) identified teleconnection patterns linking summertime precipitation variability over East Asia and North America, via a pan-Pacific wave train signal, possibly stemming from Rossby wave dispersion from fluctuations of large-scale heat sources and sinks in the Indo-Pacific region, such as El Niño. To explore the relationship with the TP, we define the TPI and the Rocky Mountain index (RMI), which is defined as 2-m temperature anomaly averaged over the region bounded by 32°–45°N, 110°–125°W. The domain selections for both the TPI and the RMI are based on the maximum T2m anomalies shown in Fig. ES1. The May TPI and May RMI from 1981 to 2015 have a correlation of −0.44 (Fig. 4a). These out-of-phase
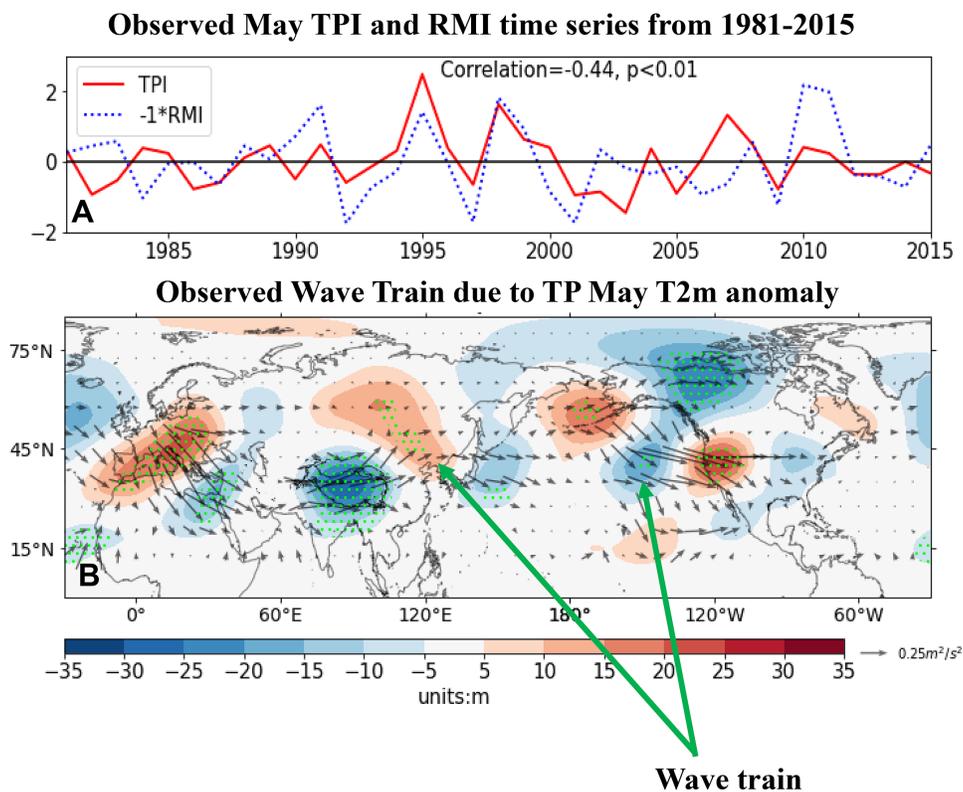

Fig. 4. Linkage between the TP and North America. (a) TPI and RMI time series. (b) Wave train. The plot in (b) is the regression of May 200-hPa geopotential height (m) of NCEP Reanalysis I from 1981 to 2015 onto (−1) times the normalized May TPI and corresponding wave activity flux (WAF; $m^2 s^{-2}$). In (b) the shading denotes the geopotential height, and vectors denote the WAF.

oscillations of TPI and RMI are significant at $p < 0.01$. Here we would like to emphasize that the significant negative correlation between TPI and RMI does not depend on the TPI domain selection. Table ES3 shows the correlations between RMI and different domains used to define TPI. Every selection has significant negative correlation, but the one defined here has the highest correlation. Moreover, both TPI and RMI areas correspond to the first mode of the maximum covariance analysis (MCA), which delineates the relationship between May T2m in TP and Rocky Mountain and June precipitation in their respective downstream regions (Xue et al. 2018).

Variations of the May 200-hPa geopotential height (GHT) associated with May TPI are further analyzed using linear regression analysis (von Storch and Zwiers 1999; Härdle and Simar 2019). The change of the 200-hPa GHT in each grid cell is calculated by regressing GHT onto the normalized TPI. The regression pattern of the 200-hPa GHT upon the TPI in May from 1981 to 2015 (Fig. 4b) demonstrates the impact on the large-scale climate dynamics manifested as a downstream wave train linking the TP to North America. The existence of such wave train is further confirmed by the regression analyses of wave flux activity (Takaya and Nakamura 2001) based on the May TPI. In this figure, the wave flux pattern progresses from the TP through the Bering Strait to the western part of North America. With such a wave pattern, cold-air advection by northly flow is expected in northwestern North America, contributing to the cold surface temperature anomaly there (Fig. 1a). The connection between high-latitude circulation and the midlatitude East Asian climate has been a subject of investigation by several studies (Zhang et al. 2019; Nakamura and Sato 2022), and it needs to be explored further. A more comprehensive discussion on the related mechanisms, such as how our numerical experiments produce this wave train in responding to the TP cooling and affect the circulation, will be presented in an LS4P special issue in *Climate Dynamics* in 2023.

Although the initial LS4P goal was to test whether the preliminary results from one model (Xue et al. 2018), i.e., the TP LST/SUBT effect on the lowland plains of the Yangtze River basin, could be confirmed by a multimodel ensemble, LS4P participants promptly realized a much larger-scale impact. This article reports, for the first time, that the spring land temperature anomaly in the TP has a teleconnected impact on summer precipitation S2S predictability over a number of midlatitude and tropical hotspots, comparable to those caused by oceanic anomalies, as shown by the percentage of model anomalies that are indicated in the third note of Fig. 3b's caption and in previous studies (Xue et al. 2018). Consistent results from observations (Fig. 1 and Fig. ES2) and multiple ESM experiments (Figs. 2, 3) show that improving the May TP land temperature simulation through LST/SUBT initialization over the TP allows ESMs to better predict June precipitation over hotspots, and that the LST over high-mountain areas could be a new source of S2S predictability through elevated heating. Our approach (high-mountain land temperature forcing) represents a new step in land–atmosphere interaction research, but much remains to be explored, including the path from potential predictability to practical prediction. We hope the momentum and excitement in this group from the GEWEX community will spark interest in this direction and further exploration by the broader scientific community readership, which is necessary to eventually reach the scientific consensus.

Findings from the LS4P first phase effort have stimulated similar studies over other high-elevation areas and/or different years (Yang et al. 2021; Diallo et al. 2022). The LS4P Phase II will focus on the Rocky Mountain LST/SUBT effect and the interaction between TPI and RMI. In addition to ESMs, regional climate models (RCM) with large spatial domains have also recently reported promising results in this aspect (Diallo et al. 2019; Qiu et al. 2022; Xu et al. 2022) and more follow-up studies on RCM downscaling and regionally refined model (RRM) within global ESMs (Tang et al. 2019) in S2S studies should be expected. The effects of snow and aerosols in snow in high mountains on S2S prediction will also be explored in LS4P Phase II (Qian et al. 2011; Lau et al. 2018). The LS4P research is supported by decadal measurements

over the TP. With a recognition of the importance of high-mountain areas in S2S prediction, we suggest that similar measurements should be made in other high-elevation regions.

Data availability statement. The CMA observational datasets are available from http://data.cma.cn/en. CRU datasets are available from https://crudata.uea.ac.uk/cru/data/hrg/cru_ts_4.05/. CAMS datasets are available from https://psl.noaa.gov/data/gridded/data.ghcncams.html. Reanalysis 1 is available from https://psl.noaa.gov/data/gridded/data.ncep.reanalysis.html. All simulation datasets are available from http://data.tpdc.ac.cn/en/. See Xue et al. (2021) for download instruction.

References

Barlow, M., S. Nigam, and E. H. Berbery, 2001: ENSO, Pacific decadal variability, and U.S. summertime precipitation, drought, and stream flow. *J. Climate*, **14**, 2105–2128, https://doi.org/10.1175/1520-0442(2001)014<2105:EPDVAU>2.0.CO;2.

Barnett, T. P., L. Dümenil, U. Schlese, E. Roeckner, and M. Latif, 1989: The effect of Eurasian snow cover on regional and global climate variations. *J. Atmos. Sci.*, **46**, 661–686, https://doi.org/10.1175/1520-0469(1989)046<0661:TEOESC>2.0.CO;2.

Charney, J., W. J. Quirk, S. Chow, and J. Kornfield, 1977: A comparative study of the effects of albedo change on drought in semi-arid regions. *J. Atmos. Sci.*, **34**, 1366–1385, https://doi.org/10.1175/1520-0469(1977)034<1366:ACSOTE>2.0.CO;2.

Diallo, I., Y. Xue, Q. Li, F. De Sales, and W. Li, 2019: Dynamical downscaling the impact of spring western US land surface temperature on the 2015 flood extremes at the southern Great Plains: Effect of domain choice, dynamic cores and land surface parameterization. *Climate Dyn.*, **53**, 1039–1061, https://doi.org/10.1007/s00382-019-04630-6.

——, ——, Q. Chen, X. Ren, and W. Guo, 2022: Effects of spring Tibetan Plateau land temperature anomalies on early summer floods/droughts over the monsoon regions of South East Asia. *Climate Dyn.*, **125**, 259–265, https://doi.org/10.1007/s00382-021-06053-8.

Han, S., C. Shi, B. Xu, S. Sun, T. Zhang, L. Jiang, and X. Liang, 2019: Development and evaluation of hourly and kilometer resolution retrospective and real-time surface meteorological blended forcing dataset (SMBFD) in China. *J. Meteor. Res.*, **33**, 1168–1181, https://doi.org/10.1007/s13351-019-9042-9.

Härdle, W. K., and L. Simar, 2019: *Applied Multivariate Statistical Analysis.* 5th ed. Springer, 555 pp.

Hu, Q., and S. Feng, 2004: A role of the soil enthalpy in land memory. *J. Climate*, **17**, 3633–3643, https://doi.org/10.1175/1520-0442(2004)017<3633:AROTSE>2.0.CO;2.

Kirtman, B., and Coauthors, 2014: The North American Multimodel Ensemble: Phase-1 seasonal-to-interannual prediction; phase-2 toward developing intraseasonal prediction. *Bull. Amer. Meteor. Soc.*, **95**, 585–601, https://doi.org/10.1175/BAMS-D-12-00050.1.

Koster, R. D., and Coauthors, 2004: Regions of strong coupling between soil moisture and precipitation. *Science*, **305**, 1138–1140, https://doi.org/10.1126/science.1100217.

Lau, K.-M., and H. Weng, 2002: Recurrent teleconnection patterns linking summertime precipitation variability over East Asia and North America. *J. Meteor. Soc. Japan*, **80**, 1309–1324, https://doi.org/10.2151/jmsj.80.1309.

——, J. Sang, M. K. Kim, K. M. Kim, R. D. Koster, and T. J. Yasunari, 2018: Impacts of snow darkening effects by light absorbing aerosols on hydro-climate of Eurasia during boreal spring and summer. *J. Geophys. Res. Atmos.*, **123**, 8441–8461, https://doi.org/10.1029/2018JD028557.

Li, X., and Coauthors, 2020: CASEarth Poles: Big data for the three poles. *Bull. Amer. Meteor. Soc.*, **101**, E1475–E1491, https://doi.org/10.1175/BAMS-D-19-0280.1.

Liu, Y., Y. Xue, Q. Li, D. Lettenmaier, and P. Zhao, 2020: Investigation of the variability of near-surface temperature anomaly and its causes over the Tibetan Plateau. *J. Geophys. Res. Atmos.*, **125**, e2020JD032800, https://doi.org/10.1029/2020JD032800.

Materia, S., and Coauthors, 2022: Summer temperature response to extreme soil water conditions in the Mediterranean transitional climate regime. *Climate Dyn.*, **58**, 1943–1963, https://doi.org/10.1007/s00382-021-05815-8.

Meehl, G. A., L. Goddard, G. Boer, R. Burgman, and G. Branstator, 2014: Decadal climate prediction: An update from the trenches. *Bull. Amer. Meteor. Soc.*, **95**, 242–267, https://doi.org/10.1175/BAMS-D-12-00241.1.

Merryfield, W. J., and Coauthors, 2020: Current and emerging developments in subseasonal to decadal prediction. *Bull. Amer. Meteor. Soc.*, **101**, E869–E896, https://doi.org/10.1175/BAMS-D-19-0037.1.

Nakamura, T., and T. Sato, 2022: A possible linkage of Eurasian heat wave and East Asian heavy rainfall in relation to the rapid Arctic warming. *Environ. Res.*, **209**, 112881, https://doi.org/10.1016/j.envres.2022.112881.

Orth, R., and S. I. Seneviratne, 2017: Variability of soil moisture and sea surface temperatures similarly important for climate in the warm season. *J. Climate*, **30**, 2141–2162, https://doi.org/10.1175/JCLI-D-15-0567.1.

Pegion, K., and Coauthors, 2019: The Subseasonal Experiment (SubX): A multimodel subseasonal prediction experiment. *Bull. Amer. Meteor. Soc.*, **100**, 2043–2060, https://doi.org/10.1175/BAMS-D-18-0270.1.

Qian, Y., M. G. Flanner, L. R. Leung, and W. Wang, 2011: Sensitivity studies on the impacts of Tibetan Plateau snowpack pollution on the Asian hydrological cycle and monsoon climate. *Atmos. Chem. Phys.*, **11**, 1929–1948, https://doi.org/10.5194/acp-11-1929-2011.

Qiu, Y., J. Feng, J. Wang, Y. Xue, and Z. Xu, 2022: Memory of land surface and subsurface temperature (LST/SUBT) initial anomalies over Tibetan Plateau in different land models. *Climate Dyn.*, https://doi.org/10.1007/s00382-021-05937-z, in press.

Robertson, A. W., S. J. Camargo, A. Sobel, F. Vitart, and S. Wang, 2018: Summary of workshop on sub-seasonal to seasonal predictability of extreme weather and climate. *npj Climate Atmos. Sci.*, **1**, 20178, https://doi.org/10.1038/s41612-017-0009-1.

Scaife, A. A., and Coauthors, 2009: The CLIVAR C20C project: Selected twentieth century climate events. *Climate Dyn.*, **33**, 603–614, https://doi.org/10.1007/s00382-008-0451-1.

Schubert, S., and Coauthors, 2009: A U.S. CLIVAR project to assess and compare the responses of global climate models to drought-related SST forcing patterns: Overview and results. *J. Climate*, **22**, 5251–5272, https://doi.org/10.1175/2009JCLI3060.1.

Seager, R., L. Goddard, J. Nakamura, N. Henderson, and D. E. Lee, 2014: Dynamical causes of the 2010/11 Texas–northern Mexico drought. *J. Hydrometeor.*, **15**, 39–68, https://doi.org/10.1175/JHM-D-13-024.1.

Shukla, J., and Y. Mintz, 1982: Influence of land-surface evaporation on the Earth's climate. *Science*, **215**, 1498–1501, https://doi.org/10.1126/science.215.4539.1498.

Takaya, K., and H. Nakamura, 2001: A formulation of a phase-independent wave-activity flux for stationary and migratory quasigeostrophic eddies on a zonally varying basic flow. *J. Atmos. Sci.*, **58**, 608–627, https://doi.org/10.1175/1520-0469(2001)058<0608:AFOAPI>2.0.CO;2.

Tang, Q., and Coauthors, 2019: Regionally refined test bed in E3SM Atmosphere Model version 1 (EAMv1) and applications for high-resolution modeling. *Geosci. Model Dev.*, **12**, 2679–2706, https://doi.org/10.5194/gmd-12-2679-2019.

Trenberth, K. E., W. G. Branstator, and P. A. Arkin, 1988: Origins of the 1988 North American drought. *Science*, **242**, 1640–1645, https://doi.org/10.1126/science.242.4886.1640.

Vitart, F., 2017: Madden–Julian oscillation prediction and teleconnections in the S2S database. *Quart. J. Roy. Meteor. Soc.*, **143**, 2210–2220, https://doi.org/10.1002/qj.3079.

von Storch, H., and F. W. Zwiers, 1999: *Statistical Analysis in Climate Research.* Cambridge University Press, 484 pp.

Woolnough, S. J., 2019: The Madden-Julian oscillation. *Sub-Seasonal to Seasonal Prediction: The Gap between Weather and Climate Forecasting*, A. W. Robertson and F. Vitart, Eds., Elsevier, 93–117.

Xu, H., X.-Z. Liang, and Y. Xue, 2022: Regional climate modeling to understand Tibetan heating remote impacts on East China precipitation. *Climate Dyn*, https://doi.org/10.1007/s00382-022-06266-5, in press.

Xue, Y., F. De Sales, R. Vasic, C. R. Mechoso, S. D. Prince, and A. Arakawa, 2010: Global and seasonal assessment of interactions between climate and vegetation biophysical processes: A GCM study with different land–vegetation representations. *J. Climate*, **23**, 1411–1433, https://doi.org/10.1175/2009JCLI3054.1.

——, and Coauthors, 2016a: West African monsoon decadal variability and surface-related forcings: Second West African Monsoon Modeling and Evaluation Project Experiment (WAMME II). *Climate Dyn.*, **47**, 3517–3545, https://doi.org/10.1007/s00382-016-3224-2.

——, and Coauthors, 2016b: Spring land temperature anomalies in northwestern US and the summer drought over southern Plains and adjacent areas. *Environ. Res. Lett.*, **11**, 059502, https://doi.org/10.1088/1748-9326/11/5/059502.

——, and Coauthors, 2018: Spring land surface and subsurface temperature anomalies and subsequent downstream late spring-summer droughts/floods in North America and East Asia. *J. Geophys. Res. Atmos.*, **123**, 5001–5019, https://doi.org/10.1029/2017JD028246.

——, and Coauthors, 2021: Impact of Initialized Land Surface Temperature and Snowpack on Subseasonal to Seasonal Prediction project, phase I (LS4P-I): Organization and experimental design. *Geosci. Model Dev.*, **14**, 4465–4494, https://doi.org/10.5194/gmd-14-4465-2021.

Yang, J., H. Chen, Y. Song, S. Zhu, B. Zhou, and J. Zhang, 2021: Atmospheric circumglobal teleconnection triggered by spring land thermal anomalies over West Asia and its possible impacts on early summer climate over northern China. *J. Climate*, **34**, 5999–6021, https://doi.org/10.1175/JCLI-D-20-0911.1.

Zeng, N., J. D. Neelin, K.-M. Lau, and C. J. Tucker, 1999: Enhancement of interdecadal climate variability in the Sahel by vegetation interaction. *Science*, **286**, 1537–1540, https://doi.org/10.1126/science.286.5444.1537.

Zhang, Y., T. Zou, and Y. Xue, 2019: An Arctic-Tibetan connection on subseasonal to seasonal time scale. *Geophys. Res. Lett.*, **46**, 2790–2799, https://doi.org/10.1029/2018GL081476.

Zhao, P., and Coauthors, 2018: The third atmospheric scientific experiment for understanding the Earth–atmosphere coupled system over the Tibetan Plateau and its effects. *Bull. Amer. Meteor. Soc.*, **99**, 757–776, https://doi.org/10.1175/BAMS-D-16-0050.1.